

# Lithium insertion into silver vanadium oxide, $\text{Ag}_2\text{V}_4\text{O}_{11}$

K. West <sup>a</sup>, A.M. Crespi <sup>b</sup>

<sup>a</sup> Department of Physical Chemistry, The Technical University of Denmark, 2800 Lyngby, Denmark

<sup>b</sup> Medtronic, Inc., 6700 Shingle Creek Parkway, Minneapolis, MN 55430, USA

## Abstract

Lithium insertion into the silver vanadium oxide,  $\text{Ag}_2\text{V}_4\text{O}_{11}$ , was investigated at 25 and 100 °C, and was found to be reversible throughout the composition interval  $0 < x < 7$ ,  $x$  being the composition parameter in  $\text{Li}_x\text{Ag}_2\text{V}_4\text{O}_{11}$ . Silver was found to be mobile in the oxide, and for  $0 < x < 2$  insertion of lithium is associated with reduction of silver ions to metallic silver. When lithium is extracted, silver ions re-enter the structure.

**Keywords:** Lithium; Silver; Vanadium oxide

## 1. Introduction

The silver vanadium oxide (SVO),  $\text{Ag}_2\text{V}_4\text{O}_{11}$ , plays a prominent role among the electrode materials for primary lithium batteries used to power implantable biomedical devices. In 1993, all implantable cardiac defibrillators in clinical use were powered by this battery chemistry [1], and more than 80 000 of these batteries have been implanted to date.

The voltage of the  $\text{Li}/\text{Li}_x\text{Ag}_2\text{V}_4\text{O}_{11}$  system shows the stepped decrease with degree of discharge typical of most lithium-inserting oxides. Seven Li per  $\text{Ag}_2\text{V}_4\text{O}_{11}$  unit can be inserted before the open-circuit voltage (OCV) falls below 2.0 V. The OCV curve has two plateaus where the voltage is constant over a range of compositions: from  $x=0$  to  $x=2$  (3.24 V) and from  $x=3$  to  $x=5.2$  (2.6 V) [2]. Analogous behavior is observed in low-rate discharge curves [3].

For most lithium inserting oxides, a constant voltage plateau in the e.m.f. versus composition curve is rationalized in terms of Gibbs phase rule as a coexistence region of two phases with different densities of lithium ions in the oxide lattice. In the case of the  $\text{Li}/\text{SVO}$  system, however, the role of silver must also be considered. Depending on the mobility of Ag ions compared to the timescale of the experiment, constant voltage plateaus in this system are consistent with either of two scenarios. If silver is not redistributed in the oxide lattice during the time of the experiment, Ag is considered a part of the lattice, and constant voltage indicates a region where two oxide phases coexist. If

silver is mobile the cathode becomes a three-component system, so the presence of three phases is required to obtain a constant potential [4], possibly metallic silver in contact with two oxide phases with different concentrations of Ag and Li. The coexistence of three Li, Ag intercalated phases is not considered likely. According to this thermodynamic argument, the reduction of silver could occur on either of the voltage plateaus in the e.m.f. versus composition curve, depending on the nature of the silver mobility.

To identify the plateau where the silver reduction takes place, Takeuchi and Thiebol [3] analyzed SVO samples lithiated both chemically and electrochemically. Assuming that reduced silver would not be reoxidized during dissolution of the oxide in sulfuric acid, they found that silver reduction was associated with the 2.6 V plateau.

The structure proposed for  $\text{Ag}_{2-x}\text{V}_4\text{O}_{11}$  consists of layers of distorted edge- and corner-sharing  $\text{VO}_6$  octahedra with silver ions between the layers [2,5]. This structure can be derived from the well-known tunnel structure of the  $\beta\text{-M}_x\text{V}_2\text{O}_5$  phases by removing the  $\text{VO}_5$  pyramids from the sides of the tunnel.

The aim of the present paper is to investigate the nature and the reversibility of the lithium-insertion reaction in  $\text{Ag}_2\text{V}_4\text{O}_{11}$ .

## 2. Experimental

SVO was synthesized by a combination reaction where  $\text{Ag}_2\text{O}$  is heated with  $\text{V}_2\text{O}_5$  in a 1:2 molar ratio [2].

The composition of the product was verified by chemical analysis, and X-ray diffractogram showed only lines that could be indexed in the monoclinic unit cell of type I  $\text{Ag}_{2-x}\text{V}_4\text{O}_{11}$  [2,5].

Electrode films were prepared by casting acetonitrile suspensions of SVO and carbon (Ketjen black) on to nickel foils, with poly(ethylene oxide) (PEO) added as binder. The thickness of the electrode composite was within the range from 15 to 25  $\mu\text{m}$ . The films were dried in vacuum at 100 °C for 15 h and then at 120 °C for 1 h, before use. Cell laminates were assembled from electrode composites and lithium foils rolled on to nickel, separated either by a polymer electrolyte foil ( $\text{LiCF}_3\text{SO}_3/\text{PEO}$ ) or by liquid electrolyte ( $\text{LiClO}_4/\text{propylene carbonate (PC)}$ ) immobilized in a porous glass separator.

Electrochemical tests were performed at constant-current discharge to a fixed potential, immediately followed by a current limited potentiostatic recharge. This cycling regime has previously [6] been shown to be superior to simple constant-current cycling, as the electrode is in nearly identical states before each discharge. The amount of oxide in the cells was determined by spectrophotometric vanadium analysis after completion of cycling.

The insertion reaction was followed ex situ by X-ray diffraction. After subjection to a specified cycling regime, cells were dismantled, and the current collectors peeled off. The cell stack (including lithium electrode and polymer electrolyte) was then mounted on a glass slide and covered with Mylar foil (adhesive J-lar<sup>®</sup> tape) to avoid reactions with oxygen and moisture. The diffractogram of the laminate was then recorded on a Philips diffractometer using  $\text{Cu K}\alpha$  radiation.

### 3. Results and discussion

Fig. 1 shows voltage versus composition curves for cycling of  $\text{Li}/\text{Li}_x\text{Ag}_2\text{V}_4\text{O}_{11}$  in polymer electrolyte at 100 °C. Data are shown for the first two cycles at a rate corresponding to  $x/1.7$  h or 11 h for a full discharge. The 'differential capacity' ( $dx/dE$ ) curves plotted to the right are calculated by numerical differentiation. To obtain curves similar to cyclic voltammograms the differential capacity during recharge is plotted as positive values. At this rate, discharge of  $\text{Li}_x\text{Ag}_2\text{V}_4\text{O}_{11}$  to 2.0 V versus Li leads to insertion of 6.4 Li per formula unit. The insertion reaction is apparently reversible as it is possible to extract all inserted lithium during charge, and as re-insertion follows a voltage curve similar to that seen in the first discharge. The hysteresis between discharge and recharge curves is relatively large, but decreases after the first cycle. This is probably a consequence of the decrease in crystallite size and the increase in number of defects that is frequently the result of lithium insertion in oxides.

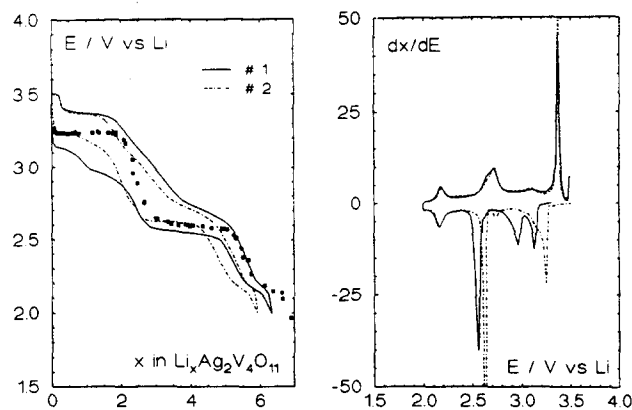


Fig. 1. First two cycles of a cell:  $\text{Li}|\text{LiCF}_3\text{SO}_3/\text{PEO}|\text{Li}_x\text{Ag}_2\text{V}_4\text{O}_{11}$  (100 °C), 25  $\mu\text{A}/\text{cm}^2$ , rate:  $x/1.7$  h). OCV data from Ref. [2] shown as solid points.

The cycling curves are compared with OCV data measured at 37 °C after three-month to one-year relaxation periods [2]. A notable difference between the dynamic curves and the OCV is the additional inflexion seen in the first discharge curve close to  $x=1$ , or more clearly as a double peak on the corresponding capacity curve. A likely origin of the additional peak is temporary insertion of lithium ions on an alternative set of sites because of slow rate of the thermodynamically preferred multi-phase reaction. This effect is suppressed in the second cycle where the kinetics apparently has improved. Allowing for distortions that can be ascribed to the kinetic properties of the insertion reaction, the two plateaus observed in the OCV curve are also represented in the voltage curves measured during cycling.

The formation of metallic silver in the SVO electrode during reduction was followed by X-ray diffraction, see Fig. 2. As the diffractograms at low diffraction angles are dominated by peaks originating from the polymer electrolyte and the Mylar cover, only data for  $2\theta$  values greater than 25° are shown. Comparison of the two lower traces in Fig. 2 shows that the Mylar cover is transparent to X-rays in this region. The low intensity of the diffractograms of the electrode composite compared with those of pristine SVO [5] is attributed to a combination of orientation effects and partial amorphization developed during the mechanical processing involved in electrode fabrication. The  $00n$  ( $n=1, 2, 3$ ) peaks of SVO are, however, enhanced by the orientation, and the 003 peak at  $2\theta=36.1^\circ$ , which has a relative intensity of  $\approx 30\%$  in pristine SVO is by far the most intense of the SVO peaks that are found in the diffractograms of electrode composites. It is clearly visible in the section of the diffractograms of electrodes prior to discharge shown in Fig. 2, the two lower traces. Electrodes discharged through the first plateau (to 3.0 V) show the appearance of three new peaks, which have positions and relative intensities characteristic of metallic silver. Reduction through the second plateau

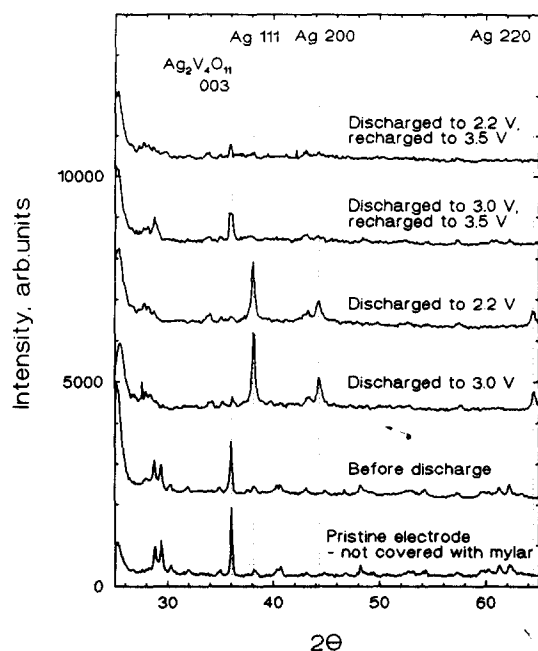


Fig. 2. Diffractograms of  $\text{Li}_x\text{Ag}_2\text{V}_4\text{O}_{11}$  electrodes after subjection to the cycling regimes indicated in the Figure. Data shown only for  $2\theta > 25^\circ$ .

(to 2.2 V) does not lead to an increase in the intensity of these peaks, and they all disappear when the electrode is recharged to 3.5 V (see Fig. 2). The 003 peak of unintercalated SVO is absent from diffractograms of discharged electrodes, but it is restored partially upon recharge. These results show that the initial step in the discharge of SVO electrodes involves reduction of the silver content of the oxide to metallic silver. The first plateau on the discharge curve thus marks the coexistence range of the phases  $\text{Ag}_2\text{V}_4\text{O}_{11}$ ,  $\text{Li}_2\text{V}_4\text{O}_{11}$  and Ag. The expulsion of silver from the oxide is fully reversible, and silver re-enters the vanadium oxide framework when the electrode is recharged to 3.5 V as can be seen both from the diffractograms and the similarity between the OCV curve and the second discharge curves. The second plateau designates a phase-separation of lithium ions within the vanadium oxide framework, i.e., coexistence of  $\text{Li}_3\text{V}_4\text{O}_{11}$  and  $\text{Li}_{5.2}\text{V}_4\text{O}_{11}$ .

The reversibility of insertion of lithium from organic electrolytes into layered hosts can be limited by co-intercalation of solvent. This is not the case with SVO, as illustrated in Fig. 3. This Figure shows voltage curves for cycling of SVO in PC/ $\text{LiClO}_4$  electrolyte at ambient temperature and a rate corresponding to  $x/2.9$  h or 19 h for a full discharge. At ambient temperature the kinetics of the insertion reaction is considerably slower than seen at  $100^\circ\text{C}$ . The first discharge in particular shows a marked hysteresis in the region where silver is reduced and expelled from the oxide lattice. Apart from that, the features of the voltage curves are the same as discussed above.

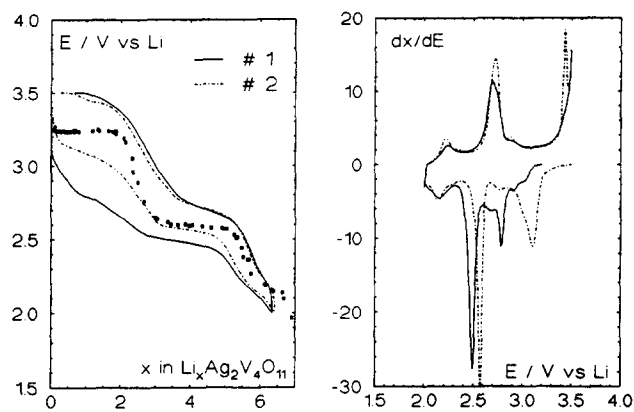


Fig. 3. First two cycles of a cell:  $\text{Li}|\text{LiClO}_4/\text{PC}|\text{Li}_x\text{Ag}_2\text{V}_4\text{O}_{11}$  ( $25^\circ\text{C}$ ,  $32 \mu\text{A}/\text{cm}^2$ , rate:  $x/2.9$  h). OCV data from Ref. [2] shown as solid points.

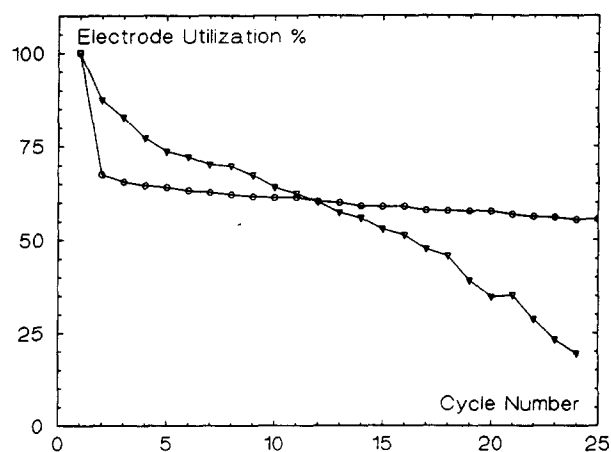


Fig. 4. Discharge capacities as function of cycle number for  $\text{Li}_x\text{Ag}_2\text{V}_4\text{O}_{11}$  electrodes discharged at ambient temperature to 2.0 V vs. Li and recharged to (—) 3.5 V and (---) 3.25 V respectively.

The data for cycling at  $100^\circ\text{C}$  (Fig. 1) shows that on the second discharge the voltage on the 2.6 V plateau is higher than the  $37^\circ\text{C}$  OCV at the same composition. The temperature dependence of the OCV ( $dE/dT$ ) must therefore be positive, because kinetic effects in the discharge data would serve only to lower the voltage. Using the voltage from the second discharge at room temperature (Fig. 3), a rough estimate of  $50 \text{ J}/(\text{mol K})$  can be obtained for the entropy, using the equation  $\Delta S = nF(\delta E/\delta T)_p$ . The results obtained for long-time cycling of SVO are biased by the fact that PC- and PEO-based electrolytes are not particularly stable at the high potentials necessary to fully recharge this material. Fig. 4 compares capacities obtained at ambient temperature with recharge to 3.25 and 3.5 V, respectively. The results are shown relative to the capacities in the first discharge (close to 6.5 Li per  $\text{V}_4\text{O}_{11}$  unit). It is seen that repeated cycling through silver reduction/oxidation leads to a much faster capacity decline than

seen in the cell that is only recharged to the composition  $\text{Li}_2\text{V}_4\text{O}_{11}$ , 2Ag.

#### 4. Conclusions

Insertion of lithium into  $\text{Ag}_2\text{V}_4\text{O}_{11}$  involves the reduction of the silver content of the oxide as well as of vanadium ions. Reduction of silver is the first step in the discharge reaction, and the reduced silver is expelled from the oxide lattice forming metallic silver particles in the electrode matrix. On oxidation, silver re-enters the oxide framework, and the insertion reaction is fully reversible in the entire composition interval  $0 < x < 7$ ,  $x$  being the composition parameter in  $\text{Li}_x\text{Ag}_2\text{V}_4\text{O}_{11}$ . Long-time cycling through the silver reduction/oxidation region leads to a fast capacity decline, probably influenced by volume changes associated with the formation/annihilation of silver particles. The stoi-

chiometric energy density calculated for lithium insertion in this material,  $\approx 730$  Wh/kg, is among the highest values reported for vanadium oxides.

#### References

- [1] C.F. Holmes, in G. Pistoia (ed.), *Lithium Batteries, New Materials, Developments and Perspectives*, Elsevier, Amsterdam, 1994, p. 377.
- [2] A.M. Crespi, P.M. Skarstad, H.W. Zandbergen and J. Schoonman, *Proc. Symp. Lithium Batteries*, Proc. Vol. 93–94, The Electrochemical Society, Pennington, NJ, USA, 1993, p. 98.
- [3] E.S. Takeuchi and W.C. Thiebolt III, *J. Electrochem. Soc.*, 135 (1988) 2691.
- [4] T. Jacobson, B. Zachau-Christiansen, K. West and S. Atlung, *Electrochim. Acta*, 34 (1989) 1473.
- [5] H.W. Zandbergen, A.M. Crespi, P.M. Skarstad and J.F. Vente, *J. Solid State Chem.*, in press.
- [6] S. Skaarup, in B.V.R. Chowdari and S. Randhkrishna (eds.), *Proc. Int. Seminar on Solid State Ionic Devices*, World Scientific Publishing, Singapore, 1988, p. 35.